Journal of Applied Fluid Mechanics, Vol. 18, No. 10, pp. 2488-2503, 2025.
Available online at www.jafmonline.net, ISSN 1735-3572, EISSN 1735-3645.
https://doi.org/10.47176/jafm.18.10.2488

Analysis of a New Blade Design for a Vertical Axis Wind Turbine Called Flow Concentrator

M. A. Carlos Alberto[1], L. G. Victor[1†], C. F. Christian[1], H. A. Isaac[2], V. P. Miriam[1] and E. M. Marco Antonio[1]

[1] *Michoacana University of Saint Nicolás of Hidalgo, Morelia, Michoacán C.P. 58000, Mexico*
[2] *National Institute of Technology of Mexico, Santiago de Querétaro, Querétaro C.P. 76000, Mexico*

†*Corresponding Author Email: victor.garza@umich.mx*

ABSTRACT

There is wind energy in urban and rural areas that is not being used sufficiently; since the wind in these areas tends to be turbulent and slow. For this reason, this study is focused on the design and analysis of a vertical axis wind turbine based on the Darrieus type, which seeks to improve self-starting, since it is one of the main problems of this type of turbine. To achieve this, the study focuses on the first stage of self-starting, also known as static torque, which occurs at an angular velocity close to zero. This stage is essential for reaching the second stage of self-starting, known as dynamic torque. To do this, a two-blade 9W Darrieus-type turbine is designed and compared with the new blade design called "flow concentrator" considering the maximum height, maximum diameter, and chord of both as constants. The analysis is performed using the Double-multiple stream tube theorem (DMST), computational fluid dynamics (CFD), and by carrying out experimental tests. The results obtained are analyzed at different wind speeds, from 3 to 8 m/s, and at different azimuthal angle positions (0°, +45°, -45°, 90°), where a considerable improvement in self-starting of up to 100% is observed in its most optimal position.

Article History

Received January 15, 2025
Revised May 7, 2025
Accepted May 27, 2025
Available online August 5, 2025

Keywords:

Self-start
Wind tunnel test
Double-multiple stream tube theorem
Micro-turbines
Computational fluid dynamics

1. INTRODUCTION

The production of electrical energy has undergone significant changes since the industrial era (Mueller, 1991). Using machines known as windmills to generate electricity has helped to significantly reduce the environmental problems of the time, and has also ushered in a wide range of improvements and revolutions not only in windmills but also in aircraft blades (Manwell, et al. 2009).

There are mainly two types of wind turbines, horizontal axis wind turbine (HAWT), which are known and used mostly for their high-power generation, but require areas with high wind speed, which are later converted into wind turbine farms but are scarce worldwide (Saad & Asmuin, 2014). On the other hand, there are also vertical axis wind turbine (VAWT) which work at low wind speeds (Saad & Asmuin, 2014). However, due to the low energy production compared to HAWT and their poor self-starting, they have been left aside in recent years, but new studies have shown that they have great potential in and around urban areas (Zibat Tasneem, et al. 2020) .

Within the VAWT there are 2 types in particular, the Savonius turbines, which work under the concept of drag forces, also have a very good self-start but have very low efficiency (Zemamou, et al. 2017), on the other hand, there are Darrieus type turbines which have two main configurations: curved blades and straight blades, called Darrieus type H (Willy, et al. 2015). The Darrieus type turbines, it presented very high efficiencies but have a very poor self-start (Paraschivoiu, 2002).

Several authors highlight the complexity of studying vertical turbines, since the constant change in angle of attack not only complicates the analysis of the operation but also the calculations of the turbine's self-start depending in its initial orientation.

The self -starting calculation is mainly defined as the torque required to overcome the moment of inertia, where the calculation of the torque in the self-starting is fundamental and can be classified as static self-starting and dynamic self-starting. The static self-starting performance refers to the torque generated at the initial azimuthal angle in which the turbine is located with an angular velocity close to zero, as shown in the study

NOMENCLATURE

c	chord	R	radius in the middle area of the turbine
C_D	airfoil drag coefficient	R_{eb}	local Reynolds number of the turbine
C_L	airfoil lift coefficient	R_{et}	turbine Reynolds number
C_N	airfoil normal coefficient	S	swept area
C_T	airfoil tangential coefficient	T	torque
D	diameter	T_{down}	downstream torque
f_{down}	downstream function	T_{up}	upstream torque
f_{up}	upstream function	u	interference factor
H	half the height	V	local wind velocity
N	blades number	V_∞	Wind stream velocity
r	local radius	ω	rotational speed
W	relative wind speed	π	Pi
X	tip speed ratio	α	local angle of attack
η	relation between the local radius and middle radius	δ	meridian angle
ρ_∞	density of the wind stream	θ	azimuthal angle
ζ	relation between the local height and the middle height		

(Xu, et al. 2024; Paraschivoiu, 2002 Wind turbine design with emphasis on Darrieus concept) for the Darrieus-H and curved blade VAWT.

On the other hand, the dynamic self-start performance is defined as the time it takes for the wind turbine to start rotating. Where (Yunus, et al. 2022; Lunt, 2005) conducts a study on a Darrieus-H VAWT where he reports that by having a TSR≥1, the turbine was in steady state and did nor reach the starting point. Khalid et al. (2022) analyzed the improvement of the dynamic self-start of a single and double Darrieus-H VAWT, for different wind speeds, where they show that two stage turbines reach the steady state faster compared to single-stage turbines. However, he mentions that its orientation significantly affects the self-start performance.

That is why there are researchers who have focused on studying the behavior of the Darrieus turbine in order to improve the self-start of the turbine through different aerodynamic profiles and their orientation (Douak & Aouachria 2015).

At the same time, these authors refer to the aerodynamic study through a two-dimensional analysis for Darrieus-H turbines, since as mentioned in (Li, et al. 2019; Xu, et al. 2024) it is suitable for the determination of the aerodynamic components. However, as mentioned by the author (Paraschivoiu, 2002, Wind turbine design with emphasis on Darrieus concept) a two-dimensional study is not suitable for a curved Darrieus turbine since the diameter of the section varies with the height, unless each section is analyzed individually as is the case with the DMST model.

Other researchers focused on the combination of Savonius turbines with Darrieus turbines looking for the most suitable configuration to improve the self-starting of the turbine, while maintaining an adequate Power Coefficient (Siddiqui et al. 2018). Other studies that have been carried out to improve self-starting are through the use of J-type aerodynamic profiles, demonstrating some improvement, but experimental tests have not yet been carried out due to the complexity of manufacturing these geometries (Zamani, et al. 2016).

In a recent study, a different blade geometry is proposed for a horizontal axis wind turbine, with the aim of improving the self-starting and the nominal power of the turbine, where thanks to this new geometry a jet effect is created that considerably improves the power and self-starting of the turbine (Casillas Farfán, et al. 2022).

Therefore, the purpose of this study is to attack the problem of self-starting of a Darrieus type VAWT, using a similar but different effect such as the nozzle effect, since the behavior of a vertical turbine is different because its angle of attack is constantly changing due to the rotation of the turbine.

For this reason, the problem is attacked by designing a new blade geometry, considering different analysis tools such as the theoretical model of the double multiple stream tube (Paraschivoiu, 2002), computational fluid dynamics CFD (ANSYS, 2024), and the experimental test (Xin, et al. 2015).

2. PROBLEM DESCRIPTION AND GEOMETRY

This study is focused on improving the initial torque of a Darrieus-type vertical axis wind turbine by creating a blade geometry Fig. 1 and 2, but, keeping the parameters of the maximum height, the maximum diameter, the chord, and the aerodynamic profile constant Fig. 4. For this purpose, the geometry of a Darrieus type blade is design and analyzed with respect to the new blade design called “Flow concentrator” using three analysis tools, through the double multiple stream tube theorem (DMST), computational fluid dynamics (CFD) and through experimental tests. The numerical modeling and simulation are carried out with the help of computer programs such as SolidWorks software, which is focused on the design of complex geometric parts such as wind turbines; Qblade software, to obtain the lift coefficient (C_L) and drag coefficient (C_D); and ANSYS software, to be able to analyze the computational fluid dynamics

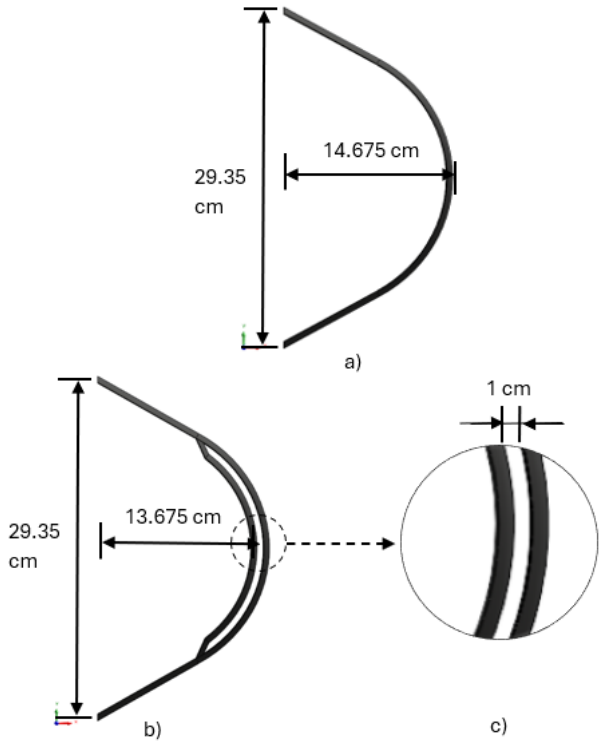

Fig. 1 Side view of blade geometry a) Darrieus blade b) Flow concentrator blade c) Middle section

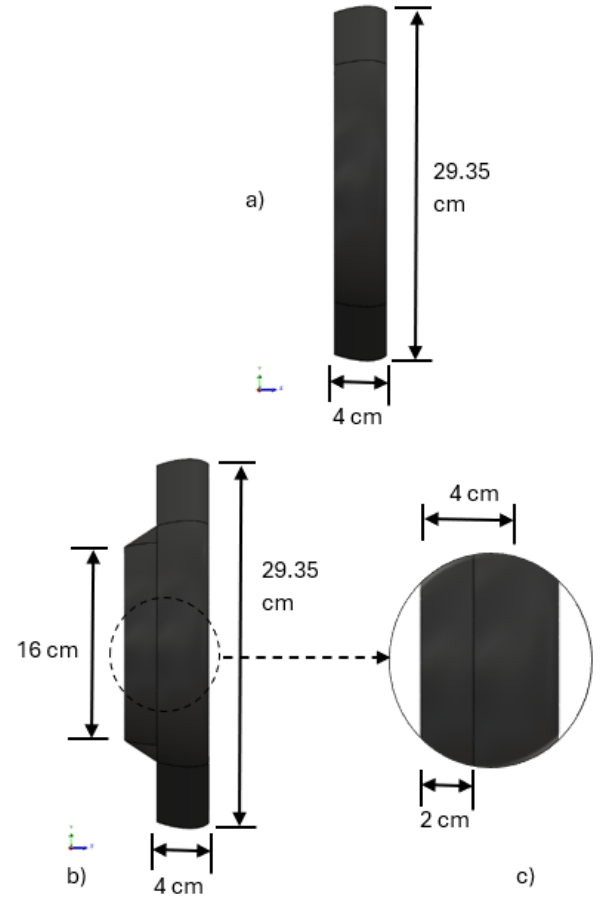

Fig. 2 Front view of blade geometry a) Darrieus blade b) Flow concentrator blade c) Middle section

Table 1 Geometrical characteristics of the turbine

Characteristic	Amount
Diameter [cm]	29.35
Radius [cm]	14.675
Heigh [cm]	29.48
Chord [cm]	4
Aerodynamic profile	Naca 6412
Number of blades	2
Wind speed [m/s]	3 – 8
Solidity	0.587
Density [kg/m^3]	1.225
Viscosity [kg/(m·s)]	1.7894e-05

(CFD) of the turbine.

The geometric dimensions of the reference Darrieus turbine are determined by the Sandia-type blade design specified in (Paraschivoiu, 2002), where the geometric characteristics of the turbine can be seen in Table 1. Where the dimensions of the wind tunnel are taken into account, these being of 60 cm high x 60 cm base, located at the University Michoacana de San Nicolas de Hidalgo.

3. METHODOLOGY

The analysis carried out is to determine the self-start of a two-blade 9W Darrieus type vertical axis wind turbine (VAWT) by calculating the initial torque and thus, designing, analyzing, and improving the self-start with a new blade geometry called "flow concentrator". This study is carried out in three parts, one using the double multi-stream tube theorem (DMST), then ANSYS Fluent software is used to carry out the study using computational fluid dynamics (CFD) and finally, the experimental tests are carried out.

3.1 Doble Multiple Stream Tube Model

The DMST is a numerical analysis model that consists of determining the upstream and downstream aerodynamic loads separately for a Darrieus and H type VAWT, Fig. (3), to calculate 2 induction factor constants, through an iterative process (Paraschivoiu, 2002), and thus consider the variation of the upstream and downstream power.

This method mentions that it is necessary to first define the geometry of the turbine to be designed, taking into account the initial parameters such as the maximum height, the maximum diameter, the number of blades, the chord, and the aerodynamic profile, as well as the wind speeds at which the analysis for the turbine's self-start is considered. These data can be seen in Table 1.

Once the design parameters have been chosen, the local Reynolds number of the turbine is determined, as shown in the Eq. (1) (Paraschivoiu, 2002).

$$Re_b = (Re_t \eta \,/\, X)\sqrt{(X - \sin\theta)^2 + \cos^2\theta \cos^2\delta} \qquad (1)$$

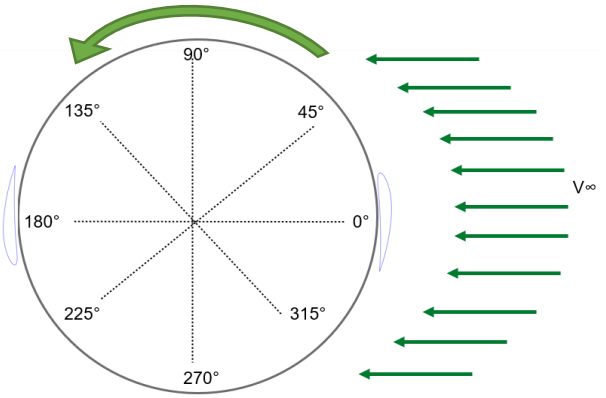

Fig. 3 Top view of the Darrieus rotor, in terms of two actuator disks

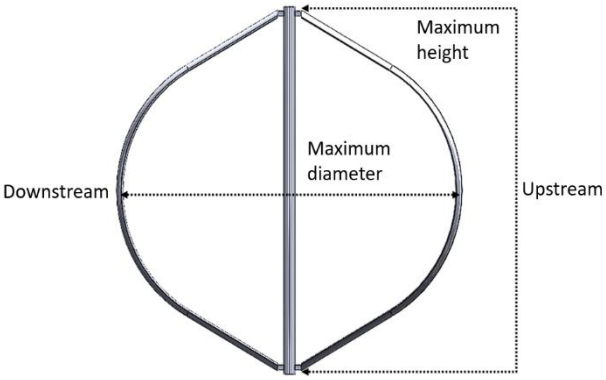

Fig. 4 Side view of the Darrieus rotor, in terms of two actuator discs

Where (X) is the ratio of the specific speed at the tip, Eq. (2), which is a function dependent on the rotational speed of the turbine and the wind speed. This rotational speed can also be represented as the revolutions per minute of the turbine; since the case of interest is self-starting, the value of the tangential speed (ω) equal to 0.1 rad/s is used to avoid errors in the calculations because there is no tangential speed before starting the turbine and, finally, the local radius (r) is used to finish the calculation.

$$X = \frac{r\omega}{V} \tag{2}$$

Subsequently, with the determination of the local Reynolds number, the most optimal angle of attack (α) observed in the aerodynamic graphs of the selected profile is chosen. Where, after the first iterative process, the angle of attack is defined by Eq. (3) where (θ *and* δ) are the azimuthal angle and the meridian angle respectively (Paraschivoiu, 2002).

$$\alpha = \sin^{-1}\left[\frac{\cos\theta\cos\delta}{\sqrt{(X-\sin\theta)^2+\cos^2\theta\cos^2\delta}}\right] \tag{3}$$

With the help of the Qblade software, the values of the lift coefficient (C_L) and the drag coefficient (C_D) are obtained, where Eq. (4) is then used to obtain the coefficient normal (C_N) and the coefficient tangential (C_T) of the aerodynamic profile (Paraschivoiu, 2002).

$$C_N = C_L\cos\alpha + C_D\sin\alpha \tag{4}$$

$$C_T = C_L\sin\alpha - C_D\cos\alpha$$

Continuing with Eq. (5), the upstream function is calculated with which a new induction factor is obtained (Paraschivoiu, 2002).

$$f_{up} = \frac{Nc}{8\pi R}\int_{-\pi/2}^{\pi/2}\left(C_N\frac{\cos\theta}{|\cos\theta|} - C_T\frac{\sin\theta}{|\cos\theta|\cos\delta}\right)\left(\frac{W}{V}\right)^2 d\theta \tag{5}$$

To obtain the new induction factor, Eq. (6) is used in order to repeat the entire iterative process until the difference between the new and the previous induction factor (u) is as small as possible (Paraschivoiu, 2002).

$$f_{up}u = \pi\eta(1-u) \tag{6}$$

When the iterative process is finished, the upstream relative velocity is calculated with Eq. (7) and with it the torque of a blade is obtained with Eq. (8) (Paraschivoiu, 2002).

$$W^2 = V^2[(X-\sin\theta)^2 + \cos^2\theta\cos^2\delta] \tag{7}$$

$$T_{up}(\theta) = \frac{1}{2}\rho_\infty cRH\int_{-1}^{1} C_T W^2(\eta/\cos\delta)\,d\zeta \tag{8}$$

Therefore, the average torque of the upstream half cycle is obtained by Eq. (9), ending the calculation in this section of the turbine (Paraschivoiu, 2002).

$$\bar{T}_{up} = \frac{N}{2\pi}\int_{-\pi/2}^{\pi/2} T_{up}(\theta)d\theta \tag{9}$$

Finally, the downstream calculation is obtained in the same way as mentioned in this section, but the initial data to perform the calculation are the final upstream data. Once both torques ($\overline{T}_{up}$) y ($\overline{T}_{down}$), are obtained, they are added together to obtain the initial torque or the theoretical self-start of the reference Darrieus type VAWT, shown in Fig. (1 and 2).

3.2. Computational Fluid Dynamics

3.2.1. Computational Domain and Boundary Conditions

In this study, a three-dimensional model is used for the CFD analysis because the Darrieus-type reference blade design chances the maximum radius with respect to the height, as does the "flow concentrator" type blade design, which, although is easier and in the case of H-type vertical turbines the analysis in two dimensions (Li, et al. 2019; Xu, et al. 2024), it would not be a more precise analysis, so it was decided to carry put the study in three dimensions.

As observed in (Alqurashi & Mohamed 2020) the orientation of the blades with respect to the wind is an important factor to consider when measuring self-starting because an initial orientation where the angle of attack is positive generates a positive torque, benefiting it. For this reason, four orientations are analyzed, these being the azimuthal angles of the turbine (0°, 45°, - 45°, 90°), with respect to the wind direction. As shown in Fig. (3 and 5). With the help of SolidWorks software, the Darrieus turbine blade geometry, and the flow concentrator blade geometry are designed, shown in Fig. (1 and 2), where the parameters for these geometries are observed in Table 1. Later, with the help of ANSYS software, two analysis

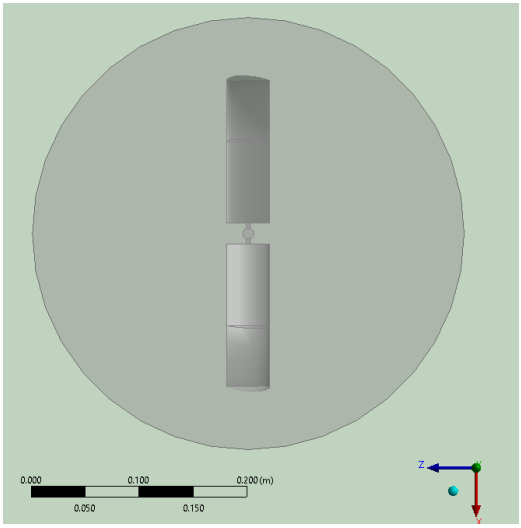

Fig. 5 Top view of conventional Darrieus Blade oriented at 0° respect to the wind speed in ANSYS

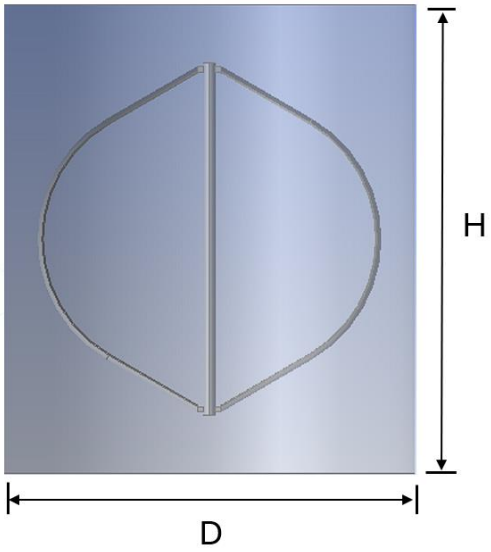

Fig. 6 Rotating zone

zones are created, which were called the rotation zone, Fig. (6), this being a cylinder that covers the turbine, which represents the turning zone of the same.

The other zone is called the wind tunnel, which has a quadrangular prism shape that contains the rotation zone and indicates the inlet and outlet flow of the wind, Fig. (7). Where the dimensions of the rotation zone and the wind tunnel are shown in Table 2, these dimensions are taken by considering the real distance between the wind tunnel and the turbine at the time of carrying out the experimental tests, and in this way, there will not be much variation between the results, as well as avoiding turbulence coming from the wind tunnel itself when simulating.

The other zone is called the wind tunnel, which has a quadrangular prism shape that contains the rotation zone and indicates the inlet and outlet flow of the wind, Fig. (7). Where the dimensions of the rotation zone and the wind tunnel are shown in Table 2, these dimensions are taken by considering the real distance between the wind tunnel and the turbine at the time of carrying out the experimental tests, and in this way, there will not be much variation between the results, as well as avoiding turbulence coming from the wind tunnel itself when simulating.

Table 2 Geometry of the analysis areas

Rotation zone		Wind tunnel	
Diameter [cm]	40	Heigh [cm]	500
Heigh [cm]	60	Base [cm]	500
		Distance upstream [cm]	400
		Distance downstream [cm]	60

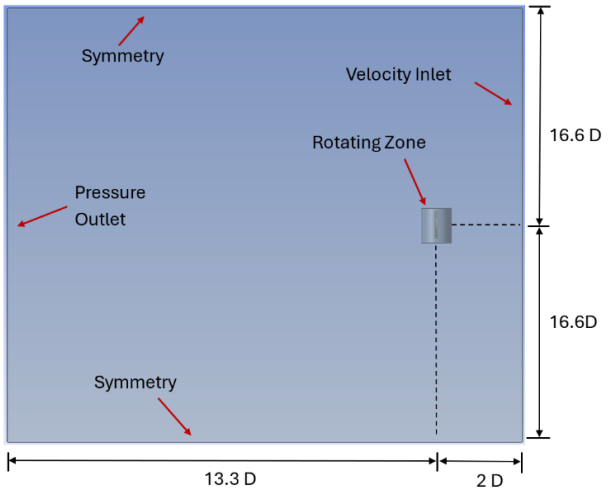

Fig. 7 Computational domain and boundary conditions

by considering the real distance between the wind tunnel and the turbine at the time of carrying out the experimental tests, and in this way, there will not be much variation between the results, as well as avoiding turbulence coming from the wind tunnel itself when simulating.

In order to compare simulation results with experimental tests more effectively and thus obtain more realistic results, certain boundary conditions are defined in the simulations. First of all, the dimensions of the wind tunnel and the rotation zone are the same for each simulation.

When performing the simulations, certain conditions are taken into account, such as the flow is incompressible, the front wall of the wind tunnel is considered as the entrance to the domain, or velocity inlet, where the airflow is always constant throughout the simulation. The back wall of the wind tunnel is considered as the outlet of the flow, or pressure outlet, the top and bottom sides are subjected to symmetry conditions, and the blade surface inside the rotating zone is set as wall boundary.

The CFD solver used is a turbulent flow solver, this being the SST model considering the curvature corrections, which was developed by Menter, which combines the formulations of the k-ω model in the near-wall zone and the k-ε model in the far region. This allows to improve the accuracy in the prediction of turbulent flows and the separation of flow under adverse pressure gradients (Menter, 1994; ANSYS, 2024), which is used by several authors in wind turbine studies due to its high quality of results obtained with respect to experimental

Table 3 Mesh analysis

Face sizing – surface blade (mm)	Number of elements	Torque (N·m)
50	289260	0.01002
25	288890	0.01000
10	289222	0.01004
5	301219	0.00996
2	1159203	0.01239
1	3980190	0.01314
0.5	14552878	0.01342

data (Casillas Farfán, et al. 2022; Xu, et al. 2024; Mohamed, 2019).

3.2.2. Governing equations

It is well known that the behavior of air around a VAWT is more complicated to understand, and in the case of a Darrieus-type turbine, it becomes even more complicated due to the change in cross-section relative to the height of the analysis. This region of airflow is governed by the Navier-Stokes equations, which describe wind motion based on the principle of conservation of mass and momentum.

The fluid flow is considered incompressible. Therefore, the simplified Navier-Stokes formulation for the conservation of mass and momentum is expressed as:

$$\nabla \cdot u = 0 \tag{10}$$

Where "u" is the velocity vector (u, v, w) in the spatial directions (x, y, z).

The momentum equations indicates that changes in fluid velocity depend on the applied forces. In its general form, it is expressed as:

$$\frac{\partial u}{\partial t} + (u \cdot \nabla)u = -\frac{1}{\rho} \cdot \nabla_p + \nu \nabla^2 u + F \tag{11}$$

Where, ρ is the air density, p is the fluid pressure, ν is the kinematic viscosity, F is the external force. These equations are solved using ANSYS Fluent software (Inc., 2024).

3.2.3. Meshing and Sensitivity Study

The mesh can be represented as a net that covers the entire area to be analyzed. Each of the sections of this net is called elements and the unions are called nodes, while finer is the net, better is the results. For this reason, the complications when simulations depend on the number of elements, the number of nodes, and their quality since they will increase both the time required and the computational resource.

The quality of the mesh depends on the geometry to be studied and is also limited mostly by the computer equipment. A very good quality mesh can have several thousand or millions of elements, which the computer equipment must solve mathematically one by one, which considerably increases the analysis time. That is why mesh analyses are carried out where the final result obtained is analyzed with respect to the number of elements and with this a decision is made as to whether the results are valid.

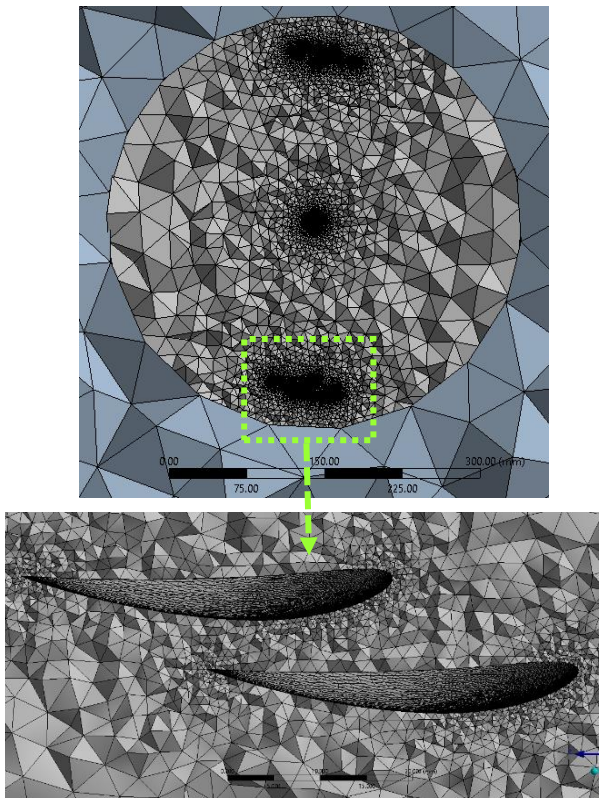

Fig. 8 Grid details for the domain

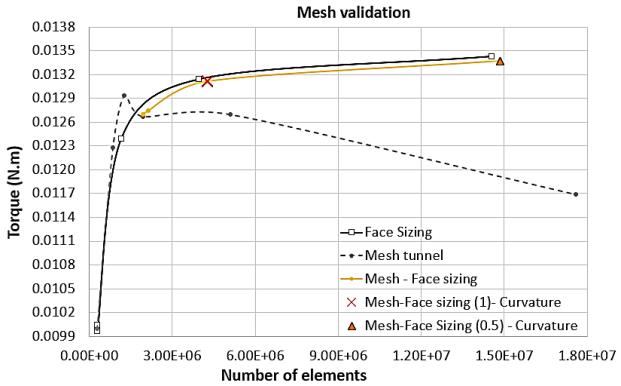

Fig. 9 Mesh validation

The mesh has a maximum element size of 100 mm for the analysis in the wind tunnel section. We use a "Face sizing" with a maximum element size of 0.5 mm for the analysis in the blade surface section, that is in the rotating zone; the curvature analysis it's used with a maximum size of 0.5 mm and the curvature is taken into account from 1 degree, it can see in Table 3. The meshing method for the rotating zone is a patch conforming composed of tetrahedral elements, as shown in Fig. (8).

In Fig. (9) the graph corresponding to the mesh validation is observed, where different mesh configurations are compared. The "Mesh tunnel" curve takes into account only the total element size for the entire analysis as an equal where the torque obtained with the variation of the mesh element from 456 mm to 25 mm is evaluated, the latter having a torque value equal to 0.0116 Nm. For "Mesh-Face sizing" curve, where an element size

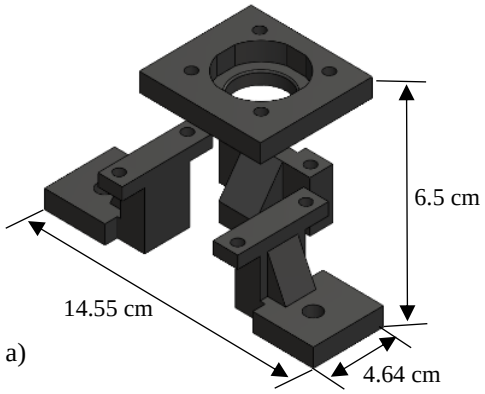

Fig. 10 a) Design of the base for the torque meter b) Mounting the base

Fig. 11 Isometric view of the assembling the 3D-printed turbine for "Flow concentrator blade"

in the tunnel of 100 mm is maintained and refining only in the turbine area from 5 mm to 0.5 mm, where for the last case a torque of 0.0133 Nm is obtained. For the case of "Mesh-Face sizing (1)-Curvature" curve, the above is analyzed, but adding the mesh to the curvature of the turbine from 10 mm to 1 mm, observing a final torque of 0.0131 Nm and for the case "Mesh-Face sizing (0.5)-Curvature" curve, the curvature is refined from 10° to 1°, observing a final torque of 0.01337 Nm.

Obtaining a variation between the last-mentioned cases of curvature of 2%, achieving the independence of the mesh in the numerical calculation.

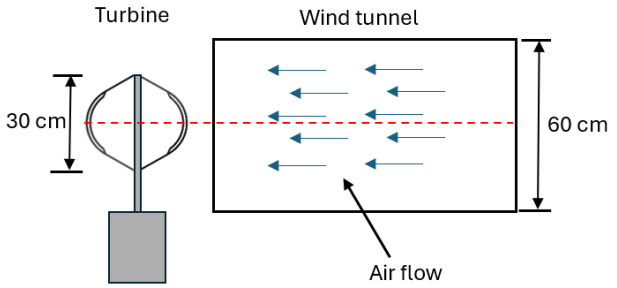

Fig. 12 Orientation of the "flow concentrator" turbine at 0° with respect to the wind tunnel

3.3. Experimental tests

In order to compare the theoretical and simulation results obtained from the reference Darrieus type blade against the new blade "flow concentrator", the experimental tests are carried out with the aid of a specialized measuring instrument, being a PCE-TM 80 torque meter, which has a resolution of 0.01 kgfcm.

Since the torque meter has a horizontal orientation, a base is designed in Fig. (10) capable of holding the turbine Fig. (11) to the torque meter and reorienting it vertically, to later mount it on a steel pillar. The design of the necessary parts for the turbine is done with SolidWorks software and they are manufactured with the help of a 3D printer, Creality 5 plus, in PLA material, with the intention of speeding up the process and keeping the costs low for self-starting tests, since what is sought is not to calculate the resistance of the turbine with respect to extreme conditions, but to obtain the aerodynamic moment.

As in the tests carried out using theoretical and simulation solutions, different experimental tests are carried out where the turbine is oriented at different azimuthal angles with respect to the wind tunnel (0°, 90°, +45°, -45° or 315°). In Fig. (12), the flow concentrator-type turbine is shown oriented at 0°, this being the case when the blade is perpendicular to the exit plane of the wind tunnel. These tests are performed for wind speed ranges from 3 m/s to 8 m/s, with increments of 1 m/s. To perform each test, the wind tunnel is turned on and the wind speed is first measured in the middle of the tunnel, which has a dimension of 60 cm base x 60 cm height, with the help of an anemometer as shown in Fig. (13).

Once the wind speed coming from the wind tunnel is obtained, the entrance is covered and then released so that the flow is completely free and even throughout the blade section. These tests are measured with the torque meter and are repeated several times at each marked speed as well as for each azimuth angle, in order to finally have a range of torques and so that the average of these results is as partial as possible.

4. RESULTS AND DISCUSSIONS

As mentioned in other sections of this research, the purpose of the study is focused on improving self-starting, so in this section, the different models, DMST, CFD, and experimental tests of the conventional Darrieus type

Fig. 13 Measuring of the wind with an anemometer

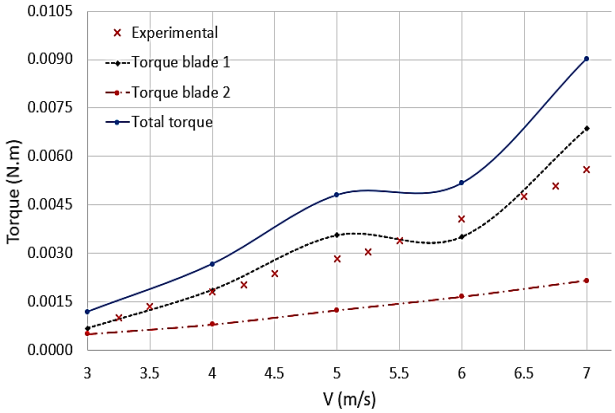

Fig. 14 Theoretical torque at 0 rad/s of the blades separately for the Darrieus turbine

turbine against the new blade geometry called "flow concentrator" are analyzed.

4.1. DARRIEUS TYPE BLADE

To make the comparison between the two blade geometries, it is first necessary to have the reference data of the conventional Darrieus-type blade and thus, establish a starting point. The Fig. (14), shows the graph of the initial torque for the Darrieus type vertical turbine, for which, the analysis is first performed using DMST, where the tangential velocity (ω) is set equal to 0.1 rad/s since, due to the equations, when designating the tangential velocity as 0, these would not be solved.

The results obtained are shown in Table 4, which shows the torque calculated for each of the speeds of interest and for each blade separately, it can be observed graphically Fig. (14). Likewise, the total torque for the turbine is oriented at an azimuthal angle of 0°, which is perpendicular to the wind tunnel as shown in Fig. (12).

Using the CFD model, the results are obtained through computational simulations using the Ansys Fluent software, which can be seen in Table 5.

Table 4 DMST model results for the Darrieus-type blade turbine

Speed m/s	Torque blade 1 (J)	Torque blade 2 (J)	Total torque (J)
3	0.00068	0.00050	0.00118
4	0.00186	0.00080	0.00266
5	0.00356	0.00124	0.00480
6	0.00350	0.00166	0.00516
7	0.00685	0.00216	0.00902

Table 5 CFD results for the Darrieus-type blade turbine

Speed (m/s)	Total torque (N.m)
3	0.00095
4	0.00171
5	0.00268
6	0.00387
7	0.00545
8	0.00715

Table 6 Experimental tests for the Darrieus-type turbine blade

Speed (m/s)	Total torque (N.m)
3	0.00068
4	0.00181
5	0.00283
6	0.00408
7	0.00560
8	0.00720

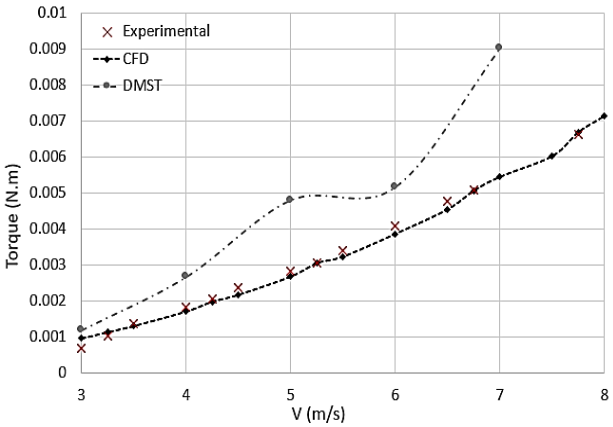

Fig. 15 Torque at 0 rad/s for the turbine with conventional Darrieus type blade, oriented at 0°

Finally, as written in the previous section, the tests carried out in the wind tunnel were to obtain the experimental data, which can be seen in Table 6.

In the graph shown in Fig. (15), the results obtained by DMST, CFD, and by experimental tests, used to obtain the initial torque of the turbine, can be observed. It is worth mentioning that these studies do not prove that the turbine will begin to rotate at any of these values, however, it can be deduced which torque tends to be generated.

Table 7 Torque obtained for the blade-type flow concentrator

Speed m/s	Total torque (J) - CFD	Total torque (J) - Experimental
3	0.00187	0.00195
4	0.00344	0.00340
5	0.00556	0.00559
6	0.00822	0.00849
7	0.01145	0.01325

The graph also shows that the data obtained using the model double multiple stream tube (DMST) tend to be above the experimental data, which was expected since this model considers ideal conditions.

It is worth mentioning that since the Reynolds number ranges between $1x10^{-4}$ to $1x10^{-3}$, the analytical process is complicated because the lift coefficient and the drag coefficient are obtained through graphs obtained in the Qblade software, which show certain anomalies due to the software's algorithm with respect to low Reynolds, leading to the hypothesis that the ideal conditions of the model and the anomalies of the coefficients due to low Reynolds generate a percentage variation of the model (DMST) with respect to the experimental tests of 27% to a maximum of 75%.

On the other hand, the curve in the graph corresponding to the CFD results is smoother and more uniform with respect to the wind speeds, where almost a convergence between the experimental and simulation results is observed. Having a minimum percentage variation of -3% for the analysis at 7 m/s and a maximum variation of -6% for the analysis at 4 m/s. The temperature and humidity during the experimental tests are recorded, observing that there was no considerable variation between tests, thus ruling out that the variation in the results was due to this cause. Another possible reason could be due to the turbulence model used in the software which in the same way was the one that gave the results closest to the experimental tests.

4.2. BLADE-TYPE FLOW CONCENTRATOR

Once the results of the different analytical models for the Darrieus type blade have been obtained, it was possible to have a reference point when carrying out the tests for the flow concentrator type blade geometry. Subsequently, the tests were carried out using CFD, which uses the same meshing considerations, shown in Table 3.

In the Table 7, it shows the comparison between the different torques obtained using the CFD method and experimental tests, shown in Fig. (16). When analyzing the results, a considerable improvement can be seen compared to the results seen in Table 6.

The double multiple stream tube model (DMST) cannot be solved because the equations shown in the previous section (3.1) are not suitable for this type of blade geometry, since the cross-section considered in this model in the middle part of the blade could be considered double and parallel to the external section of the same, causing it to be generalized and a variation between the angles existing between the two profiles cannot be obtained.

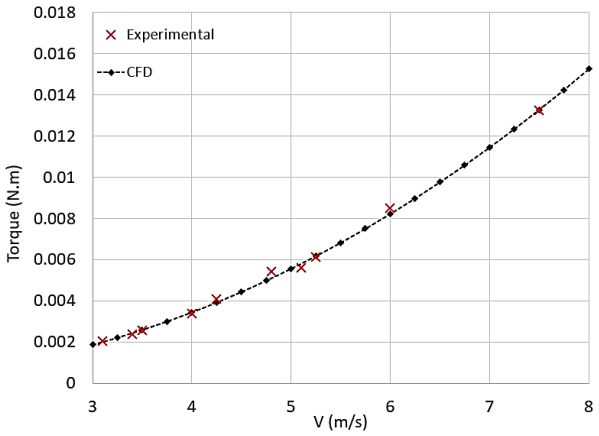

Fig. 16 Torque at 0 rad/s for the turbine with a blade-type flow concentrator, oriented a 0°

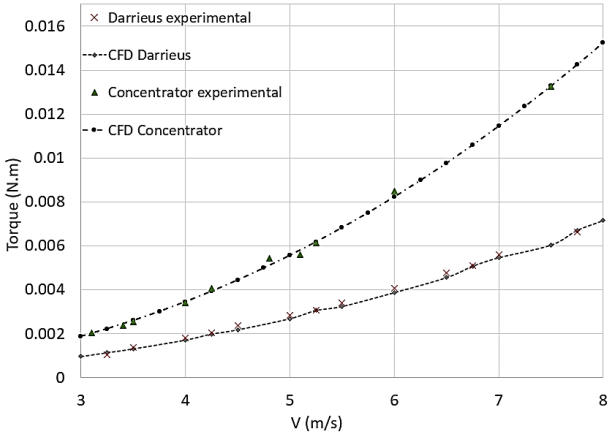

Fig. 17 Comparison of Torque at 0 rad/s at 0°, between the two blade geometries

The Fig. (17), shows the comparison of the CFD models and the experimental tests for the turbine type Darrieus and the flow concentrator type. Both turbines are analyzed under the same conditions and at the same times to avoid significant differences due to temperature and humidity, keeping the experimental tests as homogeneous as possible.

When analyzing the results obtained for both turbines using the CFD model, which are references for an orientation at 0°, it is observed that the turbine with a flow concentrator type blade presents a quite significant improvement in the initial torque, well above what was expected since at 3 m/s there is an improvement of 96% with respect to the conventional Darrieus type turbine, and improving this percentage to a maximum of 113% at 6 m/s, where it subsequently declines but still having an improvement of 98% at 7.5 m/s.

The experimental results confirm this great advantage between the new design and the conventional since there is a 100% improvement at 3 m/s, where it subsequently drops to 88% improvement at 4 m/s, but it increases again

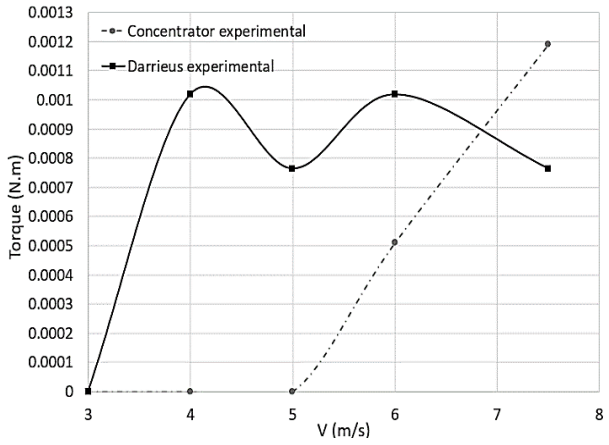

Fig. 18 Comparison of Torque at 0 rad/s at 90°, between the two blade geometries

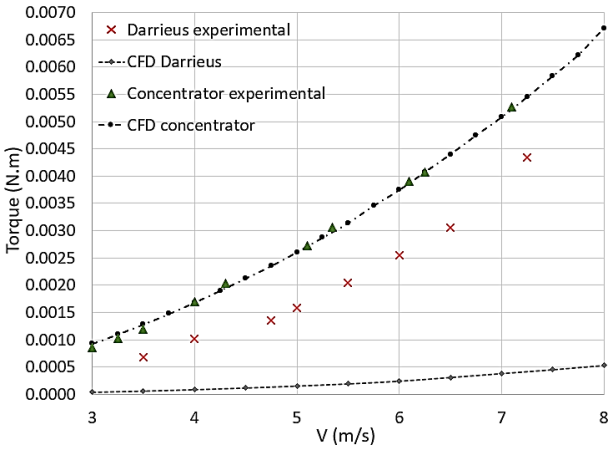

Fig. 19 Comparison of Torque at 0 rad/s at +45°, between the two blade geometries

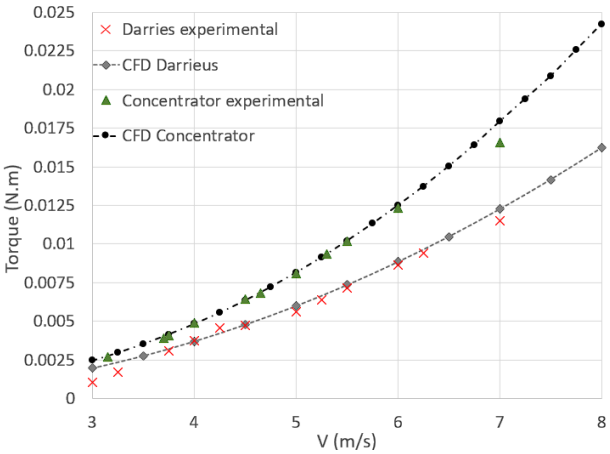

Fig. 20 Comparison of Torque at 0 rad/s at -45°, between the two blade geometries

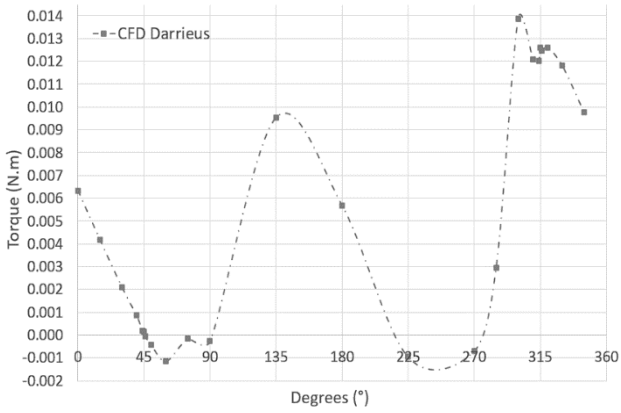

Fig. 21 Comparison of Torque at 0 rad/s at +45°, between the two blade geometries

to 108% at 6 m/s and ends with a 100% of improvement at 7.5 m/s. These experimental results show a favorable improvement in the initial torque at different wind speeds, from 3 to 7.5 m/s, for an orientation at 0°.

The Fig. (18), shows the graph of the experimental results obtained from the two turbines oriented at 90° with respect to the wind direction, where it can be seen that the turbine with the flow concentrator blades has a low initial torque between 3 and 5 m/s, unlike the turbine with the Darrieus blade. However, from 7 m/s onwards, an improvement can be seen for the blade flow concentrator. This indicates that despite having a lower initial torque at low wind speeds, from 6 m/s onwards it begins to increase drastically, where it would be necessary to carry out a study at higher wind speeds to analyze if this phenomenon continues to increase at higher speeds, which would be a fundamental factor when choosing the blade geometry for the different turbine sizes.

The Fig. (19), shows the graph of the results obtained with the tests carried out experimentally and by CFD at +45°, from 3 m/s to 8 m/s.

Where it can be observed that for the results with CFD, at all wind speeds the results referring to the flow concentrator blade type show a quite notable improvement of up 2450% at 3 m/s, however, although it is a quite favorable result and no change or error is found in the parameters of the CFD method, it is deduced that it is due to the software's algorithm at low Reynolds.

To rectify the above, we proceed to analyze the experimental data where a 25% improvement is shown for the turbine with a flow concentrator blade compared to the Darrieus type turbine at 3 m/s and obtaining a maximum improvement of 71 % at 5 m/s. Where a quite favorable result is noted experimentally and this orientation must be taken into account at higher Reynolds numbers.

To analyze why the results at +45° by CFD are separated from the experimental results, a simulation is carried out from 0° to 360° at 7 m/s for the Darrieus type turbine where Fig. (21) shows the data obtained where it is observed that this behavior is normal and is not an anomalous peak at the +45° orientation. On the other hand, in (Sheldahl, 1980) it is mentioned that the DMST model, which uses the Ansys Fluent program, is not the most suitable for turbines with high solidity; although in the case study, there is a solidity of 0.6, being below 1 as indicated by the author. In (Moghimi, & Motawej 2020) they use an approximation of the DMST model due to this problem, but for a turbine with a maximum height of 6 meters by a maximum radius of 3 meters.

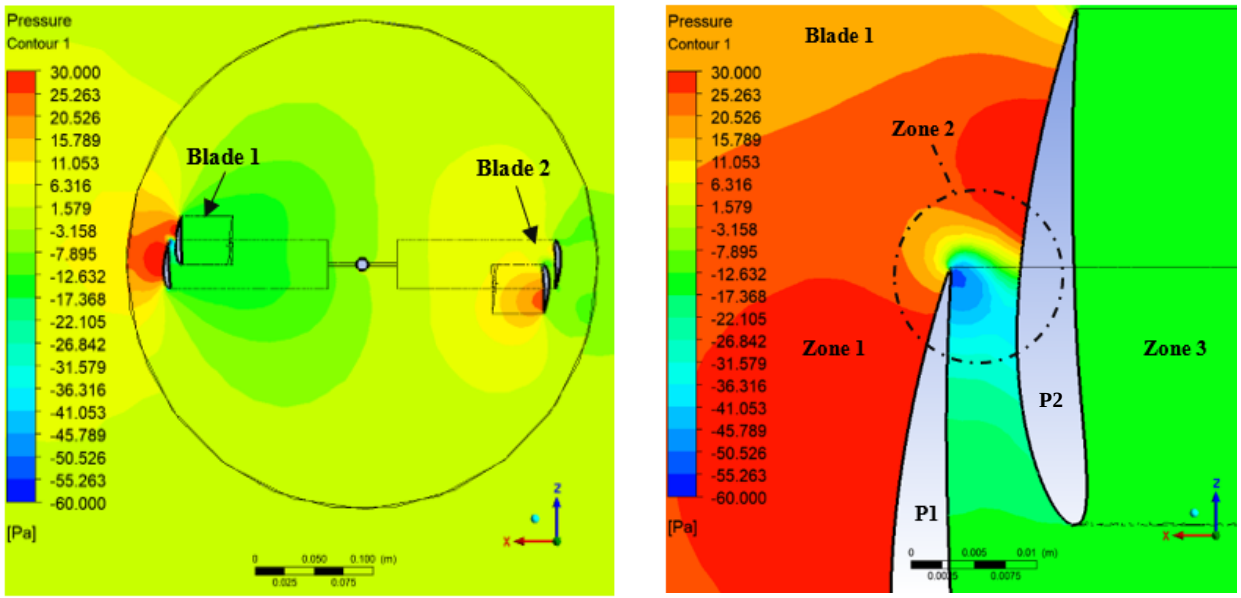

(a) (b)

Fig. 22 Cross section of the blade type Flow concentrator, oriented at 0°

In (Radu Bogateanu, 2014) a study is made for VAWTs where it is presented that at low Reynolds numbers anomalies due to wind turbulence are observed.

Due to all these factors, it is deduced that the data obtained in Fig. (19) and also observed in Fig. (21), where the results at +45° by CFD, are due to the low Reynolds number, being this of 1 x 10^3 at the ends up to 1 x 10^4 in the central area of the turbine. It is worth mentioning that the data experimentally obtained in this orientation are of great importance to further investigate the methodology of vertical turbines at low wind speeds and low Reynolds numbers.

The negative torque observed in the graph of Fig. (21), for the angles of 90° and 270°, is due to the fact that in this azimuthal position, the blades are parallel to the wind flow direction, the blade, when in this azimuthal position, is not generating any lift force, so the slight surface impact generates this negative torque. For the angles of 45° and 225°, the negative torque is due to the fact that blade 2 generates a torque greater and opposite to that obtained by blade 1. This behavior was observed only for the reference Darrieus turbine, a situation that is not observed for the "flow concentrator" blade.

In Fig. (20), the results obtained from the CFD tests for both turbines analyzed at an orientation of -45° are shown, where at 3 m/s there is an improvement in the initial torque of 30% up to a maximum of 44% at 7 m/s, in this case, it is shown how the performance of the turbine with the flow concentrator type blade improves with respect to the increase in the analyzed wind speed. In the case of the experimental tests, the same behavior is observed, starting with a 24% improvement at 3 m/s and having a constant increase until reaching 46% of improvement at 7 m/s.

4.3. PRESSURE DIFFERENTIAL

The previous section (4.2) shows that the turbine with a flow concentrator blade presents a considerable improvement in the starting torque for all the wind speeds analyzed. However, there were some doubts regarding the effect generated between the profiles, where it was considered that this intermediate hollow section could behave like a nozzle and generate an extra impulse effect due to the pressure differential that exists between the front and backside of the airfoil. For this reason, a study is carried out to be able to make a cross-section of the turbine and determine what is happening in this section.

In Fig. (22) part (a), shows a cross-section of the turbine with the blades-type flow concentrator oriented at 0°, where the airflow goes from the left side to the right side of the plane, analyzed at 7 m/s, where shows the different pressures produced in the wind tunnel and most importantly in the rotation zone.

In Fig. (22) section (b) shows in "zone 1" the pressure of 30 Pa, generated by the wind when impacting on the exposed surface of the upper surface of both profiles. In "zone 2" a vacuum pressure gradient located in the hollow area of the channel formed between both profiles "P1, P2" is shown. The vacuum pressure formed shows a pressure of -60 Pa unlike the rest of the plane, "zone 3" where the predominant pressure is between -11 Pa to -17 Pa, which also shows us a generation of a vortex that tends to induce the flow through the channel. By analyzing this point through the velocity vector flow, Fig. (24) section (b), it is conforming that vacuum pressure observed in "zone 2" Fig. (22) section (b) generates a vortex which is inducing an increase in the speed of the air that passes through the channel, the direction of the flow goes from the trailing edge, "zone 2, back", towards the leading edge of both profiles, "zone 2, front".

The vacuum pressure confirms that the wind speed inside the channel increases, causing an increase in the static torque due to the pressure gradients between both zones, generating up to 100% improvement shown in Fig. (17).

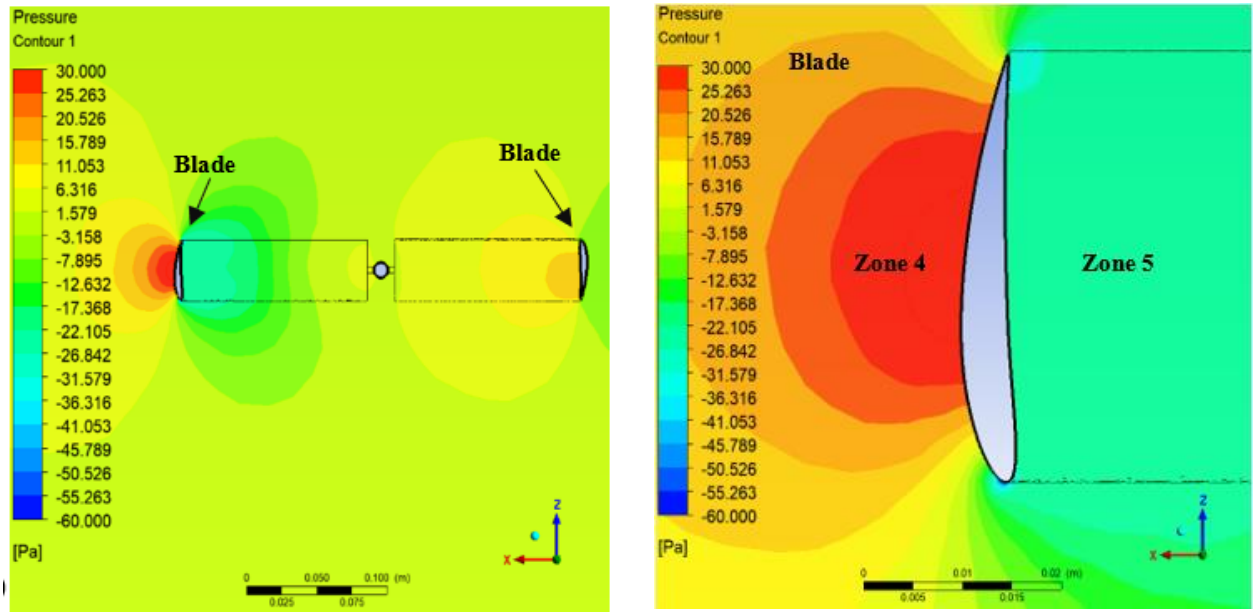

(a) (b)

Fig. 23 Cross section of the blade type Darrieus, oriented at 0°

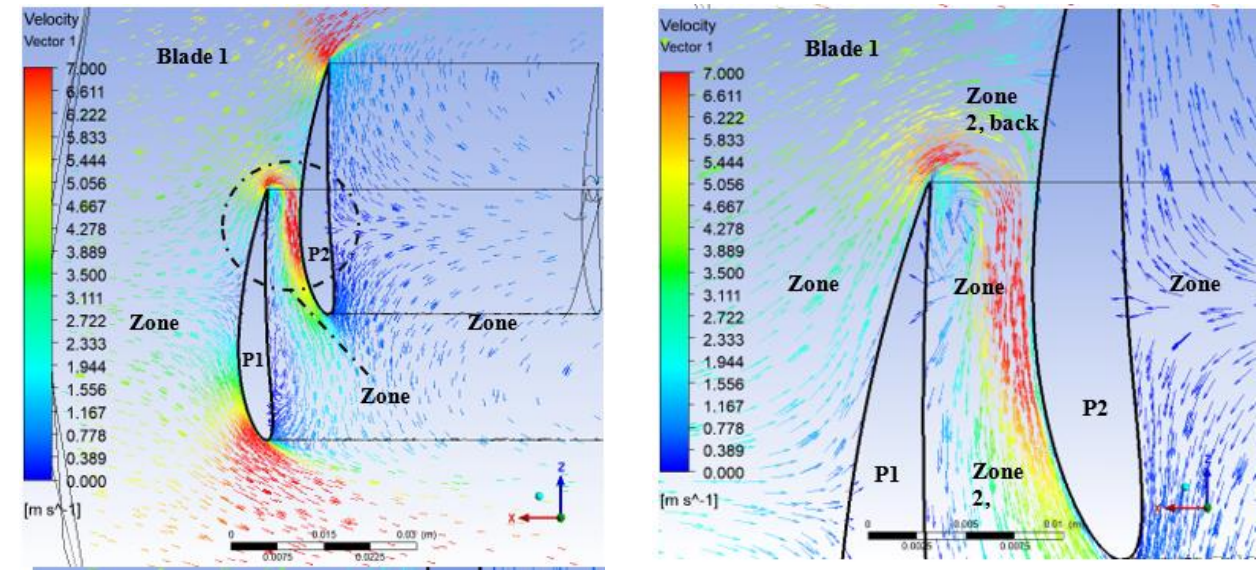

(a) (b)

Fig. 24 Velocity vectors for the blade 1 type flow concentrator, oriented at 0° at 7 m/s

In Fig. (23), shows the cross section for the Darrieus type turbine oriented at 0°, where the airflow goes from the left side to the right side of the plane, analyzed at 7 m/s. When analyzing the pressure graph for the Darrieus-type turbine, we observe in section (b) a pressure gradient from 30 Pa, on the upper surface, "zone 4", to a pressure of -7 Pa located on the lower surface "zone 5". When comparing the pressure gradients between the flow concentrator-type blade and the Darrieus blade, a greater pressure gradient is observed, which justifies the increase in static torque of the new blade geometry.

In the Fig. (25) section (a) shows the cross section of the flow concentrator type turbine, referring to blade 2, which is the rear part of the turbine oriented at 0°. The air flow goes from the lower surface “zone 6” to the upper surface of the “zone 8” profiles.

In Fig. (22) section (a) no vacuum pressure is observed in the channel formed by both profiles of blade 2, as was observed in blade 1, because blade 1 generates a wake that prevents the flow from acting on the hollow area blade 2.

When observing the plane of the velocity vectors, Fig. (25) section (b), a vortex is generated on the upper surface, “zone 7, front”, for the profile “P3”, which triggers an induction of the air flow into the channel from the leading edge “zone 7, front” of both profiles “P3, P4” towards the trailing edge “zone 7, back”, again increasing the speed of the air in the channel as a result of the contraction.

In Fig. (26) section (a), the velocity vector field of blade 1 is shown, produced by the free speed of 7 m/s for

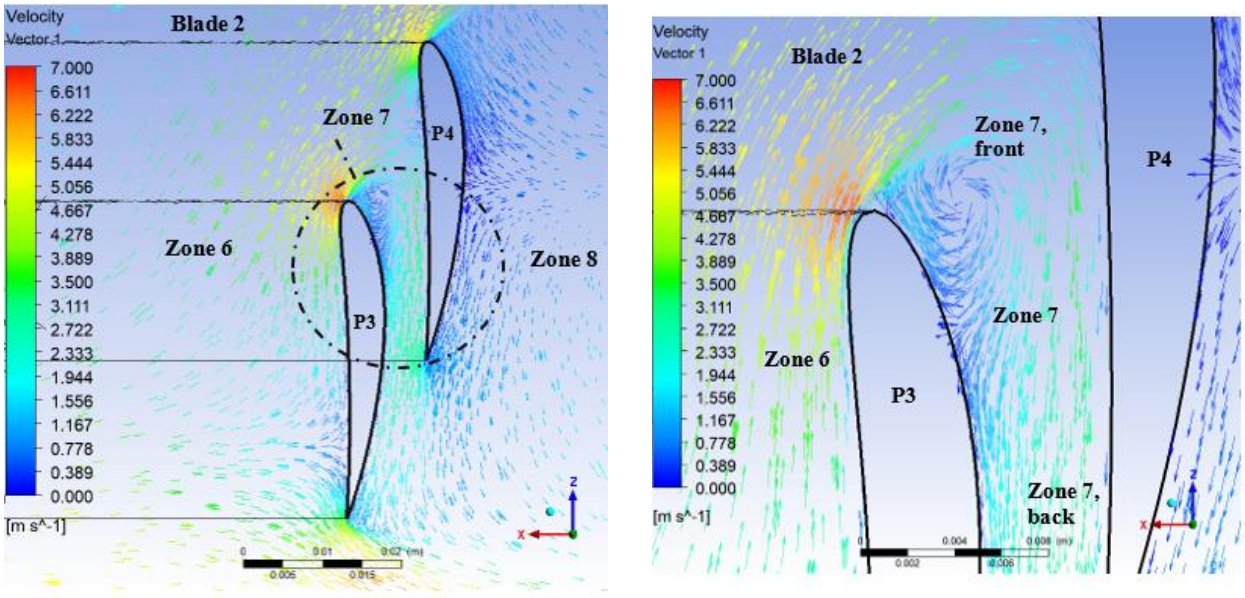

(a) (b)

Fig. 25 Velocity vectors for the blade 2 type flow concentrator, oriented at 0° at 7 m/s

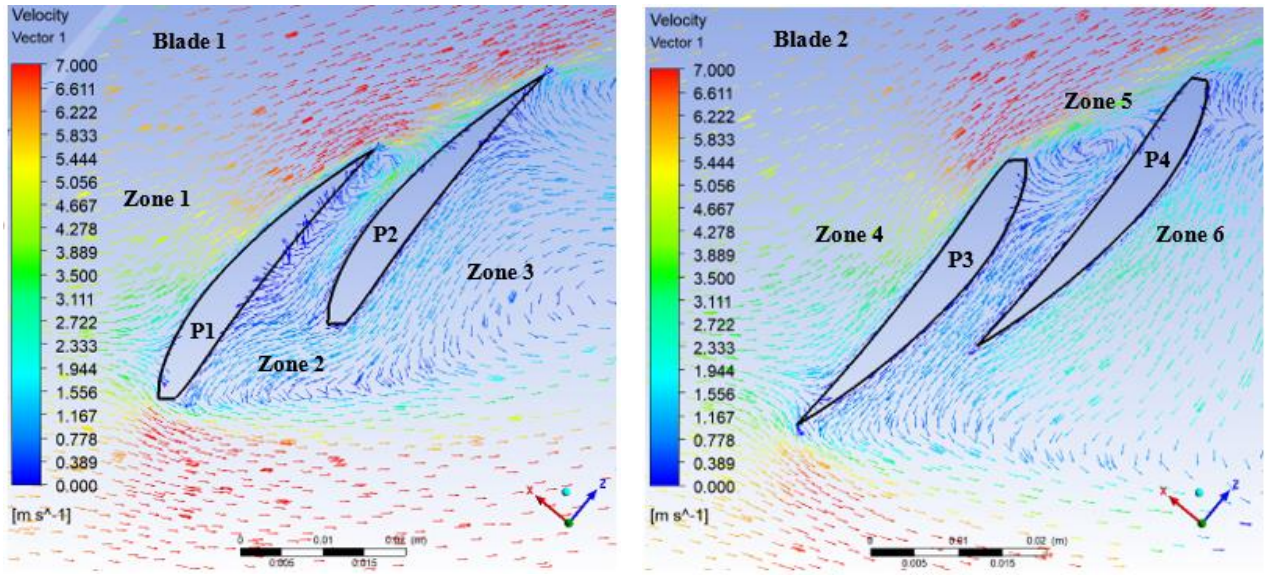

(a) (b)

Fig. 26 Velocity vectors for the blade 2 type flow concentrator, oriented at -45° or 315° at 7 m/s

the flow concentrator type turbine oriented at -45° or 315°, where the flow that goes from zone 1 to zone 3, does not produce a considerable impact on the middle zone of both profiles, zone 3, as observed in Fig. (24) for the orientation at 0°. However, it can be observed that the wake behind both profiles, zone 3, is wide, thus obtaining the expected pressure differential for the rotation of the turbine. In section (b), the velocity vector field for blade 2 is shown, where the most relevant is located in the middle zone of both profiles, zone 5, where a vortex is visualized in the leading edge, of both profiles, which unlike Fig. (25) section (b), the incident flow is of very low speed which verifies a lower static torque in this orientation as opposed to 0°.

In Fig. (27) in section (a) the velocity vector field of blade 1 is shown, for the turbine oriented at +45°, where the main observations are found in zone 2, where it is observed that the incident flow between both profiles is considerable but causes two vortices to form, one in the leading edge of profile P1 and another in profile P2, which are rotating in opposite directions, deducing that this effect reduces the pressure differential causing the final static torque at this orientation to be much lower than in the case of the turbine oriented at -45°, as also shown in the graphs, Fig. (20, 21). In section (b), the air flow for blade 2 is shown, where it is observed that the speed of the vectors passing between both profiles, zone 5, increases the speed at the free air speed.

In Fig. (28) the velocity vector field for blades 1 and 2 is shown, oriented at 90°, however, due to the chosen aerodynamic profile and the orientation of the blades, the air flow passes relatively parallel to the profiles, which

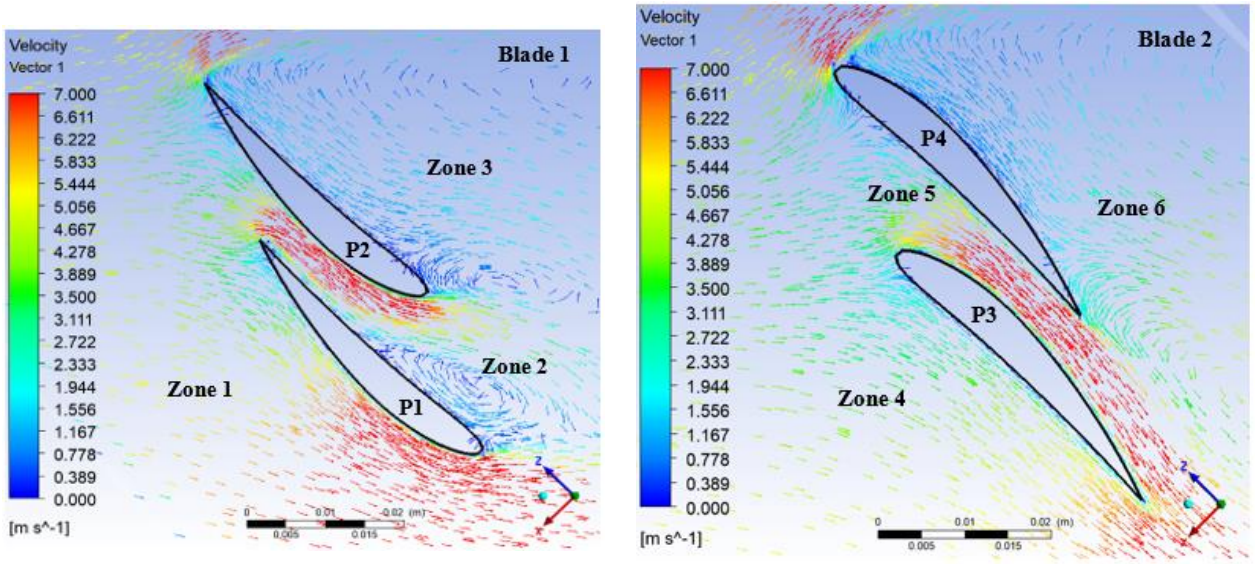

(a) (b)

Fig. 27 Velocity vectors for the blade 2 type flow concentrator, oriented at +45° at 7 m/s

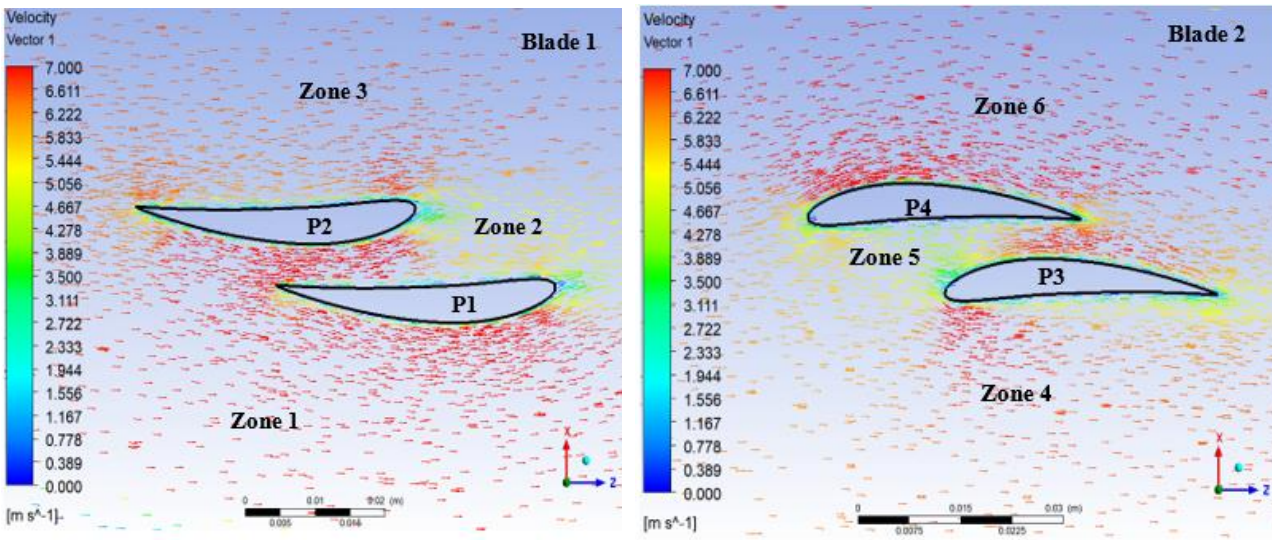

(a) (b)

Fig. 28 Velocity vectors for the blade 2 type flow concentrator, oriented at +90° at 7 m/s

does not generate a pressure differential and would explain why in the graph, Fig. (18), there are no striking changes in the static torque of the turbine.

5. CONCLUSION

It was possible to improve the self-starting of a turbine for small dimensions and low wind speeds.

To achieve this objective, a study of a Darrieus-type turbine was carried out, which is designed under the considerations mentioned in (Paraschivoiu, 2002) , and serves as a reference point to compare with the new blade geometry called "Flow Concentrator".

From the CFD simulations and experimental results for both turbines, it is concluded that:

- The same meshing conditions cannot be considered, due to the observed and mentioned turbulences.
- The experimental results show an improvement in the starting torque or torque static for the new blade geometry called flow concentrator in the four azimuthal angle orientations analyzed, having a greater impact at 0°, +45° and -45° for low wind speeds achieving an improvement between 25% up to 108%, taking as an average a 65% of improvement between the percentages of 25% and 108%, because this percentage will change depending on where the turbine is oriented with respect to the wind direction.
- In the middle section formed between the two aerodynamic profiles of the blade-type flow concentrator, a low-pressure zone is formed, causing a greater gradient pressure, which would indicate that more wind energy is being used for the same maximum dimensions as the reference Darrieus-type turbine.

- When analyzing the behavior of the velocity vectors, it is observed that the air current does indeed pass through the channel formed between both profiles for both blades, depending on the position it generates low-pressure zones that prevent a greater entry of the flow, so future research will seek to optimize the blades.
- The channel formed between both aerodynamic profiles is of interest to improve the design of the new blade geometry that uses a nozzle concept, which takes advantage of this negative pressure that proves to be an extra impulse and in the same way for future research to analyze the effect that it could generate with other conditions.

CONFLICT OF INTEREST

The authors declare that they have no competing financial interests or personal relationships that could have appeared to influence the work reported in this article.

AUTHORS CONTRIBUTION

M. A. Carlos Alberto: Methodology, Research, Original draft, Resources, Software, Design, Data analysis. **L. G. Víctor:** Methodology, Validation, Data analysis, Corrections, Obtaining equipment. **C. F. Christian**: Software, Data analysis, Corrections. **H. A. Isaac**: Methodology, Data Analysis, Observations. **V. P. Miriam**: Software, Data Analysis, Drafting. **E. M. Marco Antonio**: Methodology, Observations

REFERENCES

Alqurashi, F. & M. H. Mohamed (2020). Aerodynamic forces affecting the h-rotor darrieus wind turbine. *Hindawi Modelling and Simulation in Engineering*, *2020*, 15. https://doi.org/10.1155/2020/1368369

Casillas Farfán, C., Solorio Díaz, G. , López Garza, V., Galván González, S. & Figueroa, K. (2022). Novel induction blade design for horizontal axis wind turbines to improve starting phase: CFD and testing analysis. *Journal of Applied Fluid Mechanics*, *15*(6), 1635-1648. https://doi.org/10.47176/jafm.15.06.1163

Douak, M. & Aouachria, A. (2015). Starting torque study of darrieus wind turbine. *International Journal of Physical and Mathematical Sciences*, *9*(8). https://doi.org/10.5281/zenodo.1108332

ANSYS Inc. (2024). ANSYS Fluent User's Guide.

Khalid, M. S. U., Wood, D., & Hemmati, A. (2022). Self-starting characterics and flow induced rotation of single and dual stage vertical axis wind turbines. *Energies*, *15*. https://doi.org/10.3390/en15249365

Li, Y., Zhao, S., Qu, C., Feng, F., & Kotaro, T. (2019). Effects of offset blade on aerodynamic characteristics of small-scale vertical axis wind turbine. *Journal of Thermal Science*, *28*(2), 326 - 339. https://doi.org/10.1007/s11630-018-1058-4

Lunt, P. A. (2005). *An aerodynamic model for a vertical-axis wind turbine.* UK: MEng Project Report, School of Engineering, University of Durham.

Manwell, J. F., McGowan, J. G., & Rogers, A. L. (2009). *Wind energy explained - theory, desgin and application.* United Kingdom: John Wiley & Sons Ltd. https://doi.org/10.1002/9781119994367

Menter, F. R. (1994). Two-equation eddy-viscosity turbulence models for engineering applications. *AIAA Journal*, *32*(8), 1598-1605. https://doi.org/10.2514/3.12149

Moghimi, M., & Motawej H. (2020). Developed DMST model for performance analysis and parametric evaluation of Gorlov vertical axis wind turbines. *Sustainable Energy Technologies and Assessments*, *37*. https://doi.org/10.1016/j.seta.2019.100616

Mohamed, M. H. A. D. (2019). Blade shape effect on the behavior of the H-rotor Darrieus wind turbine: Performance investigation and force analysis. *Elservier*, *179*, 1217-1234. https://doi.org/10.1016/j.energy.2019.05.069

Mueller, T., K. (1991). Oferta y demanda de energía y electricidad: consecuencias para el medio ambiente. *Electricity and the Environment* (págs. 1-5). Helsinki: OIEA. Obtenido de https://www.iaea.org/sites/default/files/33304980913_es.pdf

Paraschivoiu, I. (2002). *Wind turbine design with emphasis on Darrieus concept.* Québec, Canada: École Polytechnique de Montréal.

Radu Bogateanu, A. D. (2014). Reynolds number efects on the aerodynamic performance of small VAWTs. *U.P.B. Sci. Bull*, *76*, 25-36. Corpus ID: 210129865

Saad, M. M. M. & Asmuin, N. (2014). comparison of horizontal axis wind turbines and vertical axis wind turbines. *IOSR Journal of Engineering*, *04*, 27-30. https://doi.org/10.9790/3021-04822730

Sheldahl, R. E., Klimas, P. C. & Feltz, L. V. (1980). Aerodynamic performance of a 5m diameter darrieus turbine. *Journal of Energy*, *4*(5), 227-232. https://doi.org/10.2514/3.48025

Siddiqui, A. S., Mian, S. N., M. Alam, M. Saleem ul Haq; A. H. Memon, & M. S. Jamil (2018). Experimental study to assess the performance of combined Savonius Darrieus vertical axis wind turbine at different arrangements. *IEEE*. https://doi.org/10.1109/INMIC.2018.8595538

Willy, T., Tjukup M., Sohif, M., M. H. Ruslan, & K. Sopian (2015). Darrieus vertical axis wind turbine for power generation I: Assesment of Darrieus VAWT configurations. *Renewable Energy*, *75*, 50-67. http://dx.doi.org/10.1016/j.renene.2014.09.038

Xin, J., Zhao, G., KeJun, G., & Wenbin, J. (2015). Darrieus vertical axis wind turbine: Basic research methods. *Renewable and Sustainable Energy Reviews*, *42*, 212-225. https://doi.org/10.1016/j.rser.2014.10.021

Xu, Z., Dong, X., Li, K., Zhou, Q. & Zhao, Y. (2024). Study of the Self-starting Performance of a Vertical-axis Wind Turbine. *Journal of Applied Fluid Mechanics*, 17(6), 1261-1276. https://doi.org/10.47176/jafm.17.6.2295

Yunus, C., D. Ingham, Lin, M., & Pourkashanian, M. (2022). Design and aerodynamic performance analyses of the self-starting H-typ VAWT having J-shaped aerofoils considering various design parameters using CFD. *Energy*, *251*. https://doi.org/10.1016/j.energy.2022.123881

Zamani, M., Maghrebi, M. J., & Varedi, S. R. (2016). Starting torque improvement using J-shaped straight-bladed Darrieus vertical axis wind turbine by means of numerical simulation. *Renewable Energy*, 109-126. https://doi.org/10.1016/j.renene.2016.03.069

Zemamou, M., Aggour, M., & Toumi, A. (2017). Review of savonius wind turbine design and performance. *Energy Procedia*, *141*, 383-388. https://doi.org/10.1016/j.egypro.2017.11.047

Tasneem, Z., Al Noman, A., Das, S. K., Saha, D. K., Islam, Md. R., Ali, Md. F., Badal, Md. F. R., Ahamed, Md. H., Moyeen, S. I.,& F. Alam (2020). An analytical review on the evaluation of wind resource and wind turbine for urban application: prospect and challenges. *Developments in the Built Environment*, *4*. https://doi.org/10.1016/j.dibe.2020.100033